

Modeling of the first indirect effect: Analysis of measurement requirements

Graham Feingold¹

Received 13 June 2003; revised 25 July 2003; accepted 10 September 2003; published 9 October 2003.

[1] We investigate the extent to which aerosol extinction is a suitable proxy for the aerosol affecting drop formation. First we use multiple realizations of a cloud model to investigate the sensitivity of cloud drop effective radius r_e to aerosol parameters (size distribution and composition) and dynamical parameters (updraft and liquid water content). In general, r_e is most sensitive to cloud liquid water, a parameter often ignored in indirect effect analyses. The relative importance of the other parameters varies for different conditions but aerosol concentration N_a is consistently important. Updraft plays an increasingly important role under high aerosol loadings. A breakdown of the individual aerosol terms contributing to drop size change shows that use of aerosol extinction as a proxy for size distribution and composition tends to underestimate the magnitude of the first indirect effect. This may influence interpretation of current satellite and surface remote measurements of the indirect effect. **INDEX TERMS:** 0305 Atmospheric Composition and Structure: Aerosols and particles (0345, 4801); 0320 Atmospheric Composition and Structure: Cloud physics and chemistry; 1610 Global Change: Atmosphere (0315, 0325); 1640 Global Change: Remote sensing. **Citation:** Feingold, G., Modeling of the first indirect effect: Analysis of measurement requirements, *Geophys. Res. Lett.*, 30(19), 1997, doi:10.1029/2003GL017967, 2003.

1. Introduction

[2] The first aerosol indirect effect [Twomey, 1977] hypothesizes that under conditions of equivalent liquid water content LWC, increased concentrations of atmospheric aerosol will result in higher concentrations of cloud condensation nuclei (CCN), increased cloud droplet concentrations, and more reflective clouds. Over the intervening decades great effort has been directed at detecting and quantifying the indirect effect using models and observations. These studies typically address the effect of aerosols on clouds in a dynamically evolving system that includes feedbacks such as aerosol-induced modifications to precipitation [Albrecht, 1989]. The constraint of constant LWC as a basis for comparison is practically difficult to achieve although attempts in this direction have been made using models [Schwartz *et al.*, 2002] and surface-based remote sensors [Feingold *et al.*, 2003]. The attempt to isolate the Twomey indirect effect from the more general indirect effect is rooted in a desire to clarify fundamental aerosol-cloud microphysical processes.

[3] In situ measurements, both surface-based and airborne, address the fundamental microphysical processes by measuring size distribution and composition. However, for climate monitoring purposes it is not feasible to perform global measurements of these parameters with the detail applied to in situ measurements. Satellites use passive remote sensors to measure aerosol optical depth τ_a which is used as an indicator of aerosol effects on cloud drop size. Satellites provide global coverage of aerosols and clouds but do not measure details of aerosol size and composition. In addition, aerosol measurements are path-integrated and not collocated with clouds. Surface based remote sensors [e.g., Feingold *et al.*, 2003] measure aerosol extinction α beneath clouds, cloud droplet size, and liquid water path (LWP) in a single column of air at scales pertinent to cloud drop formation (~ 100 m). Again, α (local τ_a) is used as a proxy for size distribution and composition.

[4] The question explored in this paper is whether proxies such as α are adequate, or alternatively, what set of measurements needs to be made to provide useful assessments of the first indirect effect. One can view this as an endeavour to guide measurement strategies in the coming years.

2. Model

[5] We use an adiabatic cloud parcel model that represents the hygroscopic growth of CCN and droplet condensation [Feingold and Heymsfield, 1992]. We focus on shallow non-precipitating stratocumulus clouds where the adiabatic assumption is a good one. Drop growth by coalescence is ignored. The model is used to determine cloud drop size distributions forming on an aerosol size distribution with prescribed composition (ammonium sulfate), in an updraft with prescribed vertical velocity w varying over the range 20 cm s^{-1} ; 300 cm s^{-1} . The aerosol size distribution $n(a)$ is represented by a unimodal lognormal distribution over the range $0.011 \text{ }\mu\text{m}$; $1.1 \text{ }\mu\text{m}$ for particle radius a . The parameters are the total particle concentration, N_a ($20 \text{ cm}^{-3} \leq N_a \leq 3000 \text{ cm}^{-3}$), the median size, r_g ($0.03 \text{ }\mu\text{m} \leq r_g \leq 0.1 \text{ }\mu\text{m}$) and the breadth parameter σ ($1.3 \leq \sigma \leq 2.2$). The range of these parameters yields 4608 input conditions.

[6] In addition, simulations are performed for aerosol exhibiting various degrees of solubility as represented by the mass fraction ϵ of ammonium sulfate, which is set at either 0.10, 0.25, 0.50, 0.75, or 1.00. Finally, simulations cover conditions where cloud top LWC is either 0.10 g m^{-3} , 0.25 g m^{-3} , or 0.50 g m^{-3} . This yields a total of 23040 simulations, with 69120 model output points.

[7] The aerosol size distribution/composition assumptions are a simplification but they do include important

¹NOAA Environmental Technology Laboratory, Boulder, Colorado, USA.

Table 1. $S(X_i) = \frac{\partial \ln r_e}{\partial \ln X_i}$ where $X_i \in (N_a, r_g, \sigma, \epsilon, w, \text{LWC})$

X_i	$S(X_i)$			All, LWC = 0.25 g m ⁻³ $w = 75 \text{ cm s}^{-1}$
	All	Clean	Polluted	
LWC	0.336	0.336	0.335	
N_a	-0.283	-0.301	-0.199	-0.299
r_g	-0.087	-0.105	-0.110	-0.086
σ	0.164	0.110	0.257	0.189
w	-0.101	-0.061	-0.169	
ϵ	-0.030	-0.029	-0.032	-0.030

“Clean” indicates $N_a < 1000 \text{ cm}^{-3}$ and “Polluted” indicates $N_a > 1000 \text{ cm}^{-3}$. Column 5 calculates $S(X_i)$ for all aerosol parameters at the indicated LWC and w . The theoretical value for $S(\text{LWC})$ is 0.333 and the lower limit of $S(N_a)$ is -0.333. Calculations are valid at RH = 65%.

parameters such as number, size, breadth, and partial solubility, and facilitate understanding of a rather complex system. The primary model output used here is the radiatively important cloud-top effective radius r_e

$$r_e = \frac{\int r^3 n(r) dr}{\int r^2 n(r) dr} = f(N_a, r_g, \sigma, \epsilon, w, \text{LWC}). \quad (1)$$

The indirect effect IE is often quantified as

$$\text{IE} = -\frac{d \ln r_e}{d \ln \alpha}, \quad (2)$$

[Feingold *et al.* 2001] where $\alpha \text{ [km}^{-1}]$ is the aerosol extinction coefficient. IE represents the relative change in r_e for a relative change in α and places less reliance on the absolute measures of parameters such as α and r_e , which is of advantage when using remote sensors. α is calculated at wavelengths $\lambda = 355 \text{ nm}$, 532 nm , and 1064 nm , and at relative humidities of 65%, 85% and 95%.

3. Results

[8] Sensitivities $S(X_i)$ are defined as

$$S(X_i) = \frac{\partial \ln r_e}{\partial \ln X_i}, \quad (3)$$

where $X_i \in (N_a, r_g, \sigma, \epsilon, w, \text{LWC})$. $S(X_i)$ are calculated using a linear regression to the logarithms of model output. Table 1 summarizes the results of $S(X_i)$ for all model output and also arbitrarily distinguishes between “Clean” and “Polluted” conditions for N_a less than or greater than 1000 cm^{-3} respectively. Under all conditions, r_e is most sensitive to LWC and relatively insensitive to ϵ . Considering $r_e \propto (\text{LWC}/N_a)^{1/3}$ (where N_a is drop concentration), one sees that the regression closely approximates the theoretical value of 1/3 for $S(\text{LWC})$. Under clean conditions, $S(N_a)$ is close to its theoretical lower limit of -1/3, indicating a high level of in-cloud activation. Sensitivity to r_g and σ under clean conditions is approximately the same (although opposite in sign) whereas $S(w)$ is small. Under polluted conditions, the relative importance of σ and w in

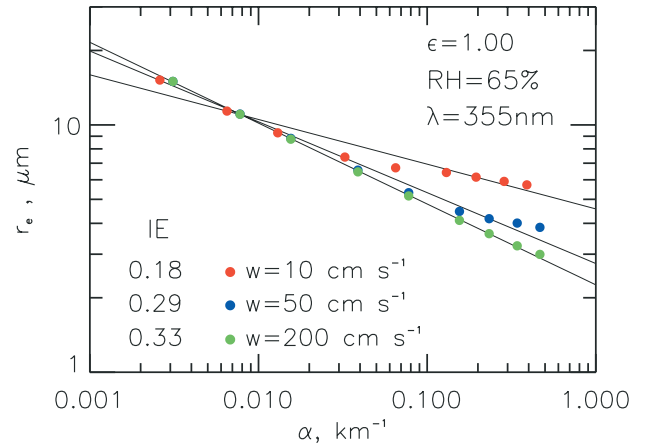


Figure 1. r_e vs. α for $r_g = 0.07 \text{ }\mu\text{m}$, $\sigma = 1.7$, $\epsilon = 1.00$, and the full range of N_a . Other conditions are noted in the legend. The slope IE is defined by Equation 2.

determining r_e increases significantly while $S(N_a)$ decreases in importance. The signs of $S(X_i)$ are as expected; specific mention is made of $S(r_g)$ where an increase in r_g results in more easily activated aerosols, higher N_d and lower r_e . $S(\sigma)$ is positive because the tail of the distribution at large sizes results in activation of larger drops, and suppression of supersaturation which tends to suppress N_d . This combination of effects makes $S(\sigma)$ quite large, particularly under polluted conditions when the larger particles are abundant [Ghan *et al.*, 1988; Feingold *et al.*, 2001]. $S(\epsilon)$ is negative because particles with higher ϵ are more easily activated, resulting in higher N_d and lower r_e .

[9] A number of graphical illustrations of these results are shown for subsets of the model output. Figure 1 shows a plot of $\ln r_e$ vs. $\ln \alpha$ for a small subsection of the model output in which all aerosol parameters but N_a are fixed. Unless otherwise stated, calculations are at $\lambda = 355 \text{ nm}$ and RH = 65%. The figure illustrates the sensitivity of IE to w at high values of α (i.e., N_a) and the eventual breakdown of a power law at high N_a and low w .

[10] Figure 2 repeats the conditions in Figure 1 but this time for a relatively insoluble aerosol with $\epsilon = 0.10$. For

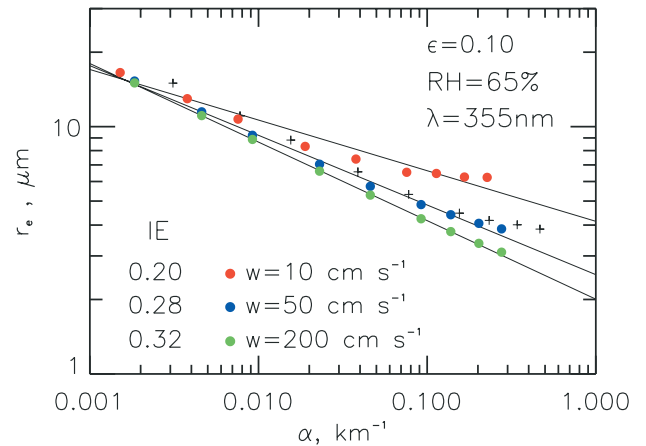


Figure 2. As in Figure 1 but for a relatively insoluble aerosol ($\epsilon = 0.10$). The crosses duplicate the results in Figure 1 at $w = 50 \text{ cm s}^{-1}$.

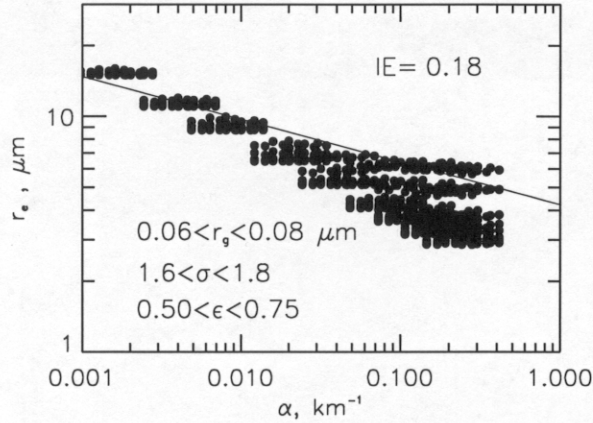


Figure 3. r_e vs. α for a range of r_g , σ , ϵ , and w . The fit is weighted by a Gaussian distribution of w , centred at $w = 0$.

comparison, the points for $w = 50 \text{ cm s}^{-1}$ from Figure 1 are superimposed on Figure 2. The lower ϵ results in lower N_a , increased r_e , and lower α but the values of IE are similar. However, the sensitivity to w is reduced somewhat.

[11] Figure 3 includes some variability in $n(a)$ and composition and for the full range of w weighted by a Gaussian distribution centred at $w = 0$, and appropriate for stratocumulus clouds. (For small cumulus, such weighting would be different since clouds will tend to form in the stronger updrafts.) One notes how the w weighting reduces IE from ~ 0.28 (as in Figures 1 and 2) to 0.18 and closer (perhaps incidentally) to remotely observed values. E.g., Nakajima *et al.* [2001] derived an IE of 0.17 over the oceans, and Bréon *et al.* [2002] measured IE = 0.04 over land and 0.085 over oceans. The largest value of IE in Feingold *et al.* [2003] at a continental site was 0.16.

[12] Finally, Figure 4 shows the full range of model output for all aerosol and dynamical conditions. The spread of points is enormous and might be representative of the range of conditions that could be encountered in the atmosphere. A fit to the points yields IE = 0.16, although this value is rather meaningless, firstly because of the enormous scatter, and secondly because of possible clustering of $n(a)$ and composition, and/or preferred LWC and w .

4. Discussion

[13] Results from these model simulations indicate that in all cases, r_e is most sensitive to LWC, a parameter often ignored in many analyses of the indirect effect. The cleaner, maritime clouds, with their high albedo contrast compared to the underlying surface are expected to be most susceptible to changes in aerosol [Platnick and Twomey, 1994]. Under clean conditions, Table 1 shows that r_e is mostly determined by LWC and N_a with decreasing dependence on σ , r_g , w , and ϵ . Under polluted conditions, the situation is more complex; N_a , σ , w and r_g all contribute significantly to r_e . Therefore requirements for measuring the indirect effect over polluted continents may be more stringent than those over cleaner, remote oceans.

4.1. Extinction vs. Size Distribution/Composition

[14] To evaluate the effectiveness of α as a proxy for the size distribution and composition we can expand Equation 2 to yield:

$$-IE' = \frac{d \ln r_e}{d \ln \alpha} = S(N_a) \frac{\partial \ln N_a}{\partial \ln \alpha} + S(r_g) \frac{\partial \ln r_g}{\partial \ln \alpha} + S(\sigma) \frac{\partial \ln \sigma}{\partial \ln \alpha} + S(\epsilon) \frac{\partial \ln \epsilon}{\partial \ln \alpha} \quad (4)$$

and calculate the individual terms based on a power-law representation of α (described below), and values of $S(X_i)$ (Table 1). The first of the four terms was considered by Twomey [1977]. We neglect the dependence of r_e on dynamical parameters since there is no direct relationship between w and α for the fixed dynamical framework considered here. (In general, a radiatively active aerosol may influence w or LWC indirectly.) We represent α as $\sim N_a^{c_1} r_g^{c_2} \sigma^{c_3} \epsilon^{c_4}$ which yields a good fit to the calculated α [Feingold *et al.* 2001]. The simple form facilitates calculation of $c_i = \partial \ln \alpha / \partial \ln X_i$; $c_i = 1.00, 3.36, 4.35$, and 0.26 for N_a , r_g , σ and ϵ , respectively, at RH = 65% and $\lambda = 355 \text{ nm}$. Coefficients $(c_i)^{-1}$ and $S(X_i)$ are then substituted into Equation 4 to calculate IE'. This is done for LWC = 0.25 g m^{-3} , $w = 75 \text{ cm s}^{-1}$, and for all aerosol conditions, and the clean and polluted conditions indicated in Table 1. The individual contributions $C(X_i) = S(X_i)/c_i$ to IE' are tabulated in Table 2. By far the largest contribution is from N_a . $C(r_g)$ and $C(\sigma)$ are relatively small while the small value of c_4 results in a fairly large $C(\epsilon)$. This contribution decreases with increasing RH (Table 2) since higher ϵ results in larger α .

[15] Table 2 also compares IE' with IE obtained directly from the regression fits to model output. IE' is always significantly higher than IE. We stress the bias rather than the absolute values because of uncertainty inherent in the regression fits. However we note that the contribution of the N_a term to IE' is itself much larger than IE from Equation 2. We have more confidence in calculations of this term because theoretically $c_i = 1$ and $S(N_a)$ is well bounded through observations. For polluted conditions, this contribution is 0.225 and happens to be the same as that suggested by Twomey (0.23). It is far larger than the direct regression

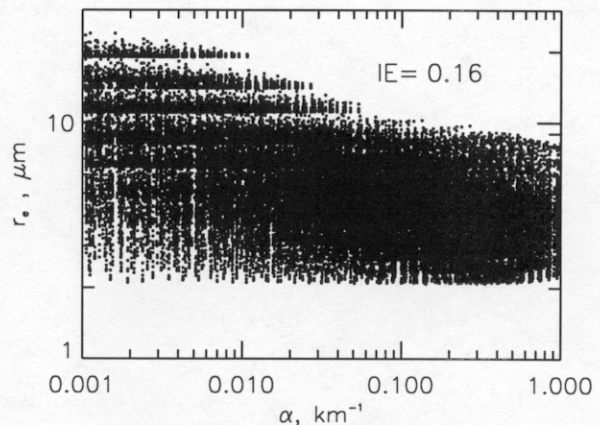


Figure 4. As in Figure 1 but for all model output points.

Table 2. Contributions $C(X_i) = S(X_i)/c_i$ to IE' (Equation 4)

	All	Clean	Polluted	RH = 95% $\lambda = 532$ nm	
				All	All
$C(N_a)$	-0.299	-0.315	-0.225	-0.299	-0.299
$C(r_g)$	-0.026	-0.024	-0.032	-0.028	-0.021
$C(\sigma)$	0.043	0.026	0.071	0.051	0.030
$C(\epsilon)$	-0.115	-0.102	-0.133	-0.049	-0.104
IE'	0.40	0.41	0.32	0.33	0.39
IE	0.16	0.14	0.03	0.17	0.13

$c_i = \frac{\partial \ln \alpha}{\partial \ln X_i} = 1.00, 3.36, 4.35,$ and 0.26 for N_a, r_g, σ and ϵ , respectively, at RH = 65% and $\lambda = 355$ nm. At RH = 95% and $\lambda = 355$ nm, $c_i = 1.00, 3.12, 3.69,$ and 0.62 . At RH = 65% and $\lambda = 532$ nm, $c_i = 1.00, 3.91, 6.33,$ and 0.29 . $IE' = \Sigma C(X_i)$. Also shown are comparisons of IE' and IE from the direct regression fit (Equation 2). LWC = 0.25 g m^{-3} and $w = 75 \text{ cm s}^{-1}$. RH = 65% and $\lambda = 355$ nm unless otherwise noted.

fit of $IE = 0.03$. Further comparison with Twomey underscores the disparity: typical relationships between N_d and N_a are $N_d \sim N_a^{0.7}$ whereas $IE = 0.03$ implies $N_d \sim N_a^{0.09}$.

[16] The above analysis suggests that ϵ may contribute to IE' . Why then is IE relatively insensitive to ϵ (cf. Figures 1 and 2)? Close examination of Figure 2 shows that increases in r_e due to low ϵ are commensurate with decreases in α due to lower hygroscopicity. As ϵ decreases, points move towards larger r_e and smaller α , approximately along the IE line (Figure 2). This conflicts with the derived contributions of ϵ in Table 2 and cautions against drawing conclusions about sensitivity of IE' to composition. Further observationally-based evaluation is called for.

5. Summary

[17] An adiabatic parcel model has been used as a tool to investigate the relative sensitivity of the radiatively important cloud drop effective radius to aerosol parameters such as number concentration, size distribution and composition, as well as to dynamic parameters such as updraft velocity and cloud water content, in non-precipitating stratocumulus clouds. It has been shown that r_e is most sensitive to LWC and that the relative importance of aerosol parameters varies as a function of aerosol loading. For similar aerosol size distributions, r_e is primarily determined by LWC and N_a under clean conditions. Under polluted conditions, the relative importance of distribution breadth, updraft velocity w and median size r_g increases significantly. This suggests that the requirements for measuring the indirect effect over polluted continents may be more stringent than those over cleaner, remote oceans. Satellite measurement of w (or proxy) may present a particular challenge.

[18] The indirect effect response is often posed as the relative change in r_e resulting from a relative change in aerosol extinction α (IE , Equation 2) [e.g., Bréon *et al.* 2002; Nakajima *et al.*, 2001; Feingold *et al.*, 2003]. This analysis suggests that three factors may affect interpretation

of those studies: (i) Lack of knowledge of LWC or liquid water path introduces ambiguity in r_e ; (ii) Updraft velocity has a strong effect on IE (Figures 1 and 2); (iii) The use of α or τ_a as a proxy for full size distribution and composition tends to underestimate IE . Examination of the individual contributions of size distribution/composition parameters to IE (Equation 4, Table 2) shows that N_a is the most significant contributor to IE . This parameter is not measured by remote sensors. Contributions from size, breadth and composition parameters appear to be of secondary importance but await direct observation for clarification of their role.

[19] The magnitudes of potential biases in IE are uncertain because they are dependent on aerosol conditions, updraft conditions and LWC, as well as our somewhat simplified analysis of the system. Nevertheless they appear to be significant enough that they may affect interpretation of surface and satellite-derived remote sensing data.

[20] **Acknowledgments.** The author acknowledges useful discussions with J. Ogren, E. Andrews, and P. Y. Chuang. This research was supported by NOAA's Climate and Global Change Research Program and by the Biological and Environmental Research Program (BER), U.S. Department of Energy, Interagency Agreement No. DE-AI03-02ER63324.

References

- Albrecht, B. A., Aerosols, cloud microphysics, and fractional cloudiness, *Science*, **245**, 1227–1230, 1989.
- Bréon, F.-M., D. Tanré, and S. Generoso, Aerosol effect on cloud droplet size monitored from satellite, *Science*, **295**, 834–838, 2002.
- Feingold, G., and A. J. Heymsfield, Parameterizations of condensational growth of droplets for use in general circulation models, *J. Atmos. Sci.*, **49**, 2325–2342, 1992.
- Feingold, G., L. A. Remer, J. Ramaprasad, and Y. Kaufman, Analysis of smoke impact on clouds in Brazilian biomass burning regions: An extension of Twomey's approach, *J. Geophys. Res.*, **106**, 22,907–22,922, 2001.
- Feingold, G., W. L. Eberhard, D. E. Veron, and M. Previdi, First measurements of the Twomey aerosol indirect effect using ground-based remote sensors, *Geophys. Res. Lett.*, **30**(6), 1287, doi:10.1029/2002GL016633, 2003.
- Ghan, S. J., G. Guzman, and H. Abdul-Razzak, Competition between sea salt and sulfate particles as cloud condensation nuclei, *J. Atmos. Sci.*, **55**, 3340–3347, 1998.
- Nakajima, T., A. Higurashi, K. Kawamoto, and J. E. Penner, A possible correlation between satellite-derived cloud and aerosol microphysical parameters, *Geophys. Res. Lett.*, **28**, 1171–1174, 2001.
- Platnick, S., and S. Twomey, Determining the susceptibility of cloud albedo to changes in droplet concentration with the advanced very high resolution radiometer, *J. Appl. Meteor.*, **33**, 334–347, 1994.
- Schwartz, S. E., Harshvardhan, and C. M. Benkovitz, Influence of anthropogenic aerosol on cloud optical properties and albedo shown by satellite measurements and chemical transport modeling, *Proc. Natl. Acad. Sci.*, **99**, 1784–1789, 2002.
- Twomey, S., The influence of pollution on the short wave albedo of clouds, *J. Atmos. Sci.*, **34**, 1149–1152, 1977.

G. Feingold, NOAA Environmental Technology Laboratory, 325 Broadway, Boulder, CO 80305, USA. (graham.feingold@noaa.gov)